Performance Comparison of Wood, Plywood, and Oriented Strand Board under High- and Low-Velocity Impact Loadings

Zahra Naghizadeh Mohammad Hossein Pol
Abiodun Oluseun Alawode Mehdi Faezipour
Gholam Hossein Liaghat Brian K. Via Ali Abdolkhani

Abstract

In this article, the behavior of wood, plywood, and oriented strand board (OSB) under high- and low-velocity impact loadings was investigated experimentally. For the high-velocity impact test, limit velocity (V_{bl}) and impact energy absorbed (E_{ab}) were determined by subjecting the material to different impact loading by conical nose projectile. For the low-velocity impact test, the materials were subjected to four levels of energy—10, 39, 78, and 98 J—and the time history responses of velocity, energy, load, and displacement were obtained. Additionally, quantitative data for damage size are presented. The results show that in comparison with OSB and solid wood plates, plywood presents better characteristics in response to both high- and low-velocity impact loadings.

Wood is commonly used as an impact energy absorber in many applications, such as packaging and containment structures surrounding systems that may disintegrate (Johnson 1986b, Reid and Peng 1997, Polocrosse et al. 2016). Under impact loading, shear failure parallel to the grain direction plays a distractive role in the failure process of solid wood. However, in laminated wood composites such as plywood and oriented strand board (OSB), the more homogenized shear strength in longitudinal and transverse directions produces a greater bending stiffness and resistance to cracking compared to solid wood (Forest Products Laboratory 2010, Otkur 2010).

Wooden materials are known to be highly strain rate sensitive (Forest Products Laboratory 2010, Otkur 2010) and become stronger and stiffer under dynamic short time loading (Task Committee on the State-of-the-Art 1975). Apart from the theoretical and numerical predictions (Deka and Vaidya 2008, Otkur 2010), limited studies are available on the experimentally measured high- and low-velocity impact behavior of wood and wood products (Naghizadeh et al. 2017, Polocoser et al. 2017). Johnson (1986a, 1986b) provided a short summary of the impact behavior of wood and briefly characterized the performance of oak planks impacted by projectiles with diameters up to 20 cm moving at 458 m/s. Douglas (1860) proposed an equation for the penetration depth induced by the impact loading in wooden structures. Inresearch done by Palamidi and Harrigan (2006), mechanical properties of balsa wood under quasi-static and dynamic loadings were investigated by a direct impact test and a Split Hopkinson Pressure Bar at high strain rates, respectively. Reid and Peng (1997) investigated the

The authors are, respectively, Postdoctoral Researcher, Forest Products Development Centre, School of Forestry and Wildlife, Auburn Univ., Auburn, Alabama (z_naghizadehmahani@yahoo.com [corresponding author]); Assistant Professor, Dept. of Mechanical Engineering, Tafresh Univ., Tafresh, Iran (m_h_pol@tafreshu.ac.ir); Postdoctoral Researcher, Forest Products Development Centre, School of Forestry and Wildlife, Auburn Univ., Auburn, Alabama (aza0236@auburn.edu); Professor, Dept. of Wood and Paper Sci. and Technol., Faculty of Natural Resources, Univ. of Tehran, Karaj, Iran (mfaezi@ut.ac.ir); Professor, Liaghat, Dept. of Mechanical Engineering, Tarbiat Moddares Univ., Tehran, Iran (ghlia530@modares.ac.ir); Professor, Forest Products Development Centre, School of Forestry and Wildlife, Auburn Univ., Auburn Alabama (brianvia@auburn.edu); and Associate Professor, Dept. of Wood and Paper Sci. and Technol., Faculty of Natural Resources, Univ. of Tehran, Karaj, Iran (abdolkhani@ut.ac.ir). This paper was received for publication in July 2021. Article no. 21-00052.

Forest Prod. J. 71(4):362–370.
doi:10.13073/FPJ-D-21-00052

dynamic response of five different types of wood by the Split Hopkinson Pressure Bar at impact velocities up to approximately 350 m/s. According to the research done by Zike and Kalnins (2011), different wood products have been subjected to drop-weight impact tests from which the lower impact resistance has been observed by particleboard and single veneer, whereas the highest energy absorption capacity was observed with seven-ply plywood made with high-density polyethylene film adhesive. Such laminates can dissipate twice the impact than that of seven-ply plywood based on phenol-formaldehyde adhesive.

To the best of our knowledge, there is no study available to compare wood and laminated wood products such as plywood and OSB in terms of high- and low-velocity impact properties. In this study, high-velocity impact tests were performed at different velocities, and the limit velocity and energy-absorbed observations were employed to compare the high-velocity impact resistance of the three materials. The behavior of the materials subjected to different levels of low-velocity impact energies was determined as well. However, it should be noted that wood materials are not very resistive against direct high-velocity loads, and they can be either used in sandwich structures or reinforced by the protective coatings. This study aimed at investigating their potentials as impact absorbers.

Materials and Methods

High-quality logs of *Alnus glutinosa* (alder) and phenol formaldehyde (PF) adhesive with pH, viscosity, solid content, and density of 12.24, 0.80 P, 41.17 percent, and 1.19 g/cm^3, respectively, were used for plywood and OSB productions. Methylene diphenyl diisocyanate (MDI) and paraformaldehyde were supplied by the Sigma-Aldrich with 98 and 95 percent purity, respectively. Paraformaldehyde, tannin powder, and 80-mesh alder wood flour were added to the adhesive as a hardener, accelerator, and filler, respectively.

Sample Preparation

Plywood

Alder veneers 2 mm thick were obtained by rotary cutting of nonsteamed logs (Aydin 2004, Aydin and Olakoglu 2005). The veneers were then dried to 6 to8 percent moisture content; 121 parts by weight of PF resin was mixed with 30, 10, 1, 10, and 17 parts of MDI, tannin, paraformaldehyde, wood flour, and water, and 200 g/m^2 of the adhesive mixture was applied on the single surfaces of each veneer. The three-layer plywood was then cold pressed for 6.3 minutes followed by a hot press at 1.08 MPa pressure and 120°C for 14 minutes. Panels produced were conditioned at 20°C and 65 percent relative humidity (RH), and cut into 53 samples of 12 by 12 by 1 cm^3 for high- and low velocity impact tests and into 10 samples for the tensile tests in accordance with ASTM D1037-13.

OSB

Alder veneers were cut into 2 by 12-cm strands for OSB production. The strands were then dried at 70°C for 48 hours to reach 2.5 percent MC and mixed with the adhesive for 6 minutes. The adhesive was a mixture of PF, MDI, tannin, paraformaldehyde, and water. The wood strands were weighed and divided into three parts and formed into a mat. The strands in the two external layers were perpendicular to the strands in the core layer. The mat was prepressed for 6.3 minutes and then pressed in a laboratory-type hot press at 1.08 MPa and 120°C for 14 minutes. Panels produced were conditioned at 20°C and 65 percent RH and cut into 53 samples of 12 by 12 by 1 cm^3 for high- and low-velocity impact tests as well as 10 samples for the tensile tests in accordance to ASTM D143.

Wood

Alder logs were sawn using a cant sawing pattern, and the tangential boards were chosen for this experiment. Dried wood panels of alder were cut into 53 samples of 12 by 12 by 1 cm^3, 33 of which were used for the high-velocity impact test and the rest for the drop weight test. Ten wood specimens were prepared for the tensile test and parallel- and perpendicular-to-grain directions, according to ASTM D805-52.

Experimental

High-velocity impact

The high-velocity impact test setup, shown in Figure 1a, consists of a long-barrel, fast-acting, high-pressure firing valve and a capture chamber. Samples were mounted in a fully clamped boundary condition between two rigid steel plates, each having a thickness of 20 mm. The eight screws were tightened to provide clamped boundary conditions, as shown in Figure 1b. The sample dimensions were governed by the specimen-holding device, which is part of the high-velocity impact test apparatus. The target unsupported area was 10 by 10 cm^2. The conical nose steel projectiles, having a mass of 9.12 g, were used in this study (Fig. 1c). The projectile was inserted into the barrel at the breech end. Next, the breech-loading system, the firing valve, and the safety bleed valve were closed. A valve placed in the breech holds the gas pressure in the pressure accumulator filled with helium gas. A gas cylinder supplies the gas to the pressure accumulator. The device was fired by opening the firing valve, which released the pressure behind the breech valve to the atmosphere. The difference in pressure opened the breech valve, allowing the high-pressure helium gas to propel the sabot mounted projectile toward the target. A pair of diode lasers and photo diodes (light-sensitive diodes) connected to a counter-timer were employed to measure the impact velocity of the projectiles (i.e., the distance between the two diodes divided by the projectile's flight time from the first diode to the second diode). After perforation, the trajectory of the projectile could be deflected. Therefore, each diode was replaced by a two-dimensional screen of parallel lasers, and photo diodes were cited in series and connected to the counter-timer, shown in Figure 1a. Each laser screen provided a larger projectile detection area compared to a single needle-thin laser beam. In order to calculate the residual velocity, the distance between the two two-dimensional screens of parallel diodes was divided by the projectile's flight time from the first screen to the second one. After completion of each test, the target was removed and inspected. The projectile was recovered from the rags. Impact velocity was varied by varying the pressure of gas in the firing chamber. Different pressure settings and impact velocities were used for the test.

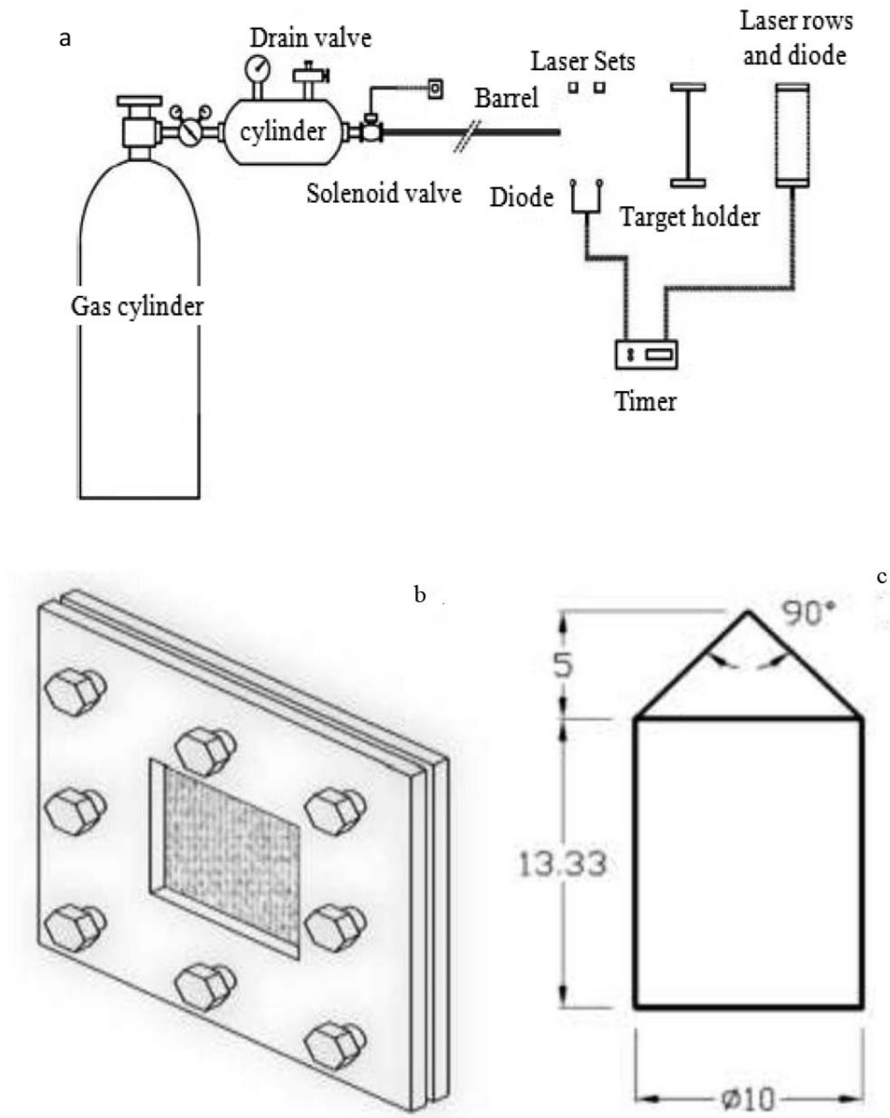

Figure 1.—Schematic representation of (a) the experimental setup for high-velocity impact tests (Pol et al. 2013), (b) sample holder (Mehrabani et al. 2016), and (c) projectile.

Low-velocity impact

A CEAST_ 9350 drop-tower low-velocity impact tester was used in this research. The test was performed by dropping a conical striker carrying a total weight of 10.045 kg on the samples from various heights. The frequency and the striker load capacity were 800 kHz and 21 kN, respectively. Four impact energy levels of 10, 39, 78, and 98 J were applied. The initial velocities for these impact energies were 1.4, 2.8, 3.95, and 4.43 m/s, and drop heights were 100, 400, 800, and 1,000 mm, respectively. The average of data for five samples as replications were taken. The testing system was capable of measuring the time history for the force $F(t)$ using the Piezo-accelerometer sensor. The system was also equipped with a laser system to measure the initial velocity.

Results and Discussion

The tensile test results are shown in Table 1. The area under the stress-strain curves was measured to calculate the toughness of the materials studied.

High-velocity impact test

Absorbed energy, as obtained by Equation 1, is one of the main parameters to assess and evaluate the degree of damage in a material after an impact,

Table 1.—Tensile test results.[a]

Sample	Ultimate strength (MPa)	CV ×	Fracture strain	CV	toughness (MPa)
B3 long	10.31	0.06	1.06	0.03	0.79
B3 trans	0.82	0.08	0.60	0.02	0.02
B2 long	1.84	0.04	0.87	0.02	0.08
B2 trans	1.92	0.07	0.52	0.02	0.03
B1 long	2.80	0.02	1.58	0.01	0.64
B1 trans	2.75	0.02	1.49	0.02	0.47

[a] B3, B2, and B1 = solid wood, oriented strand board, and plywood, respectively; long and trans = load applied parallel and perpendicular to grain directions, respectively.

$$E_{ab} = \frac{1}{2} m(V_i^2 - V_r^2) \quad (1)$$

Here, m, V_i, and V_r are the mass, initial impact velocity, and residual velocity of the projectile, respectively, and E_{ab} is the energy absorbed by the target.

Limit velocity (V_{bl}) is another parameter used to assess the performance of materials against impact loads. The limit velocity protection criteria may be defined as the average of an equal number of the highest partial penetration velocities and the lowest complete penetration velocities that occur within a specified velocity spread. In the study presented here, the initial velocity was plotted versus the residual velocity, and then the data were fitted with the Lambert-Jonas equation to estimate V_{bl} (Lambert and Jonas 1976). The following equation was proposed by Lambert and Jonas (1976) for V_{bl}:

$$V_r = \beta(V_i^P - V_{bl}^P)^{1/P} \quad (2)$$

Here, β and P are the coefficients, and V_i, V_r, and V_{bl} are the initial, the residual, and the limit velocities, respectively.

Estimated limit velocity and absorbed energy results at different impact velocity levels are shown in Table 2. Figure 2 illustrates the experimental data fitted with the Lambert-Jonas equation for solid wood, OSB, and plywood. Plywood showed relatively higher V_{bl}, 93 m/s, compared to solid wood and OSB with V_{bl}, 64 and 80 m/s, respectively. The 45 and 25 percent increases in V_{bl} were achieved with plywood and OSB composites over the solid wood, respectively. Additionally, the limit velocity in plywood is 16 percent higher than that of OSB.

Table 2.—High-velocity impact test results.

Materials	Initial velocity (m/s)	Residual velocity (m/s)	Energy absorbed (J)
Wood			
1	65	No penetration	19.27
2	71	9	22.62
3	91	48	27.25
4	100	60	29.18
5	104	65	30.05
6	109	69	32.47
7	114	73	34.96
8	146	95	56.05
9	165	105	73.87
10	175	110	84.47
11	184	115	94.08
Plywood			
1	89	No penetration	36.12
2	100	24	42.97
3	110	43	46.74
4	117	55	48.63
5	125	66	51.39
6	146	94	56.91
7	149	Error	—
8	162	Error	—
Oriented strand board			
1	72	No penetration	23.64
2	85	21	30.93
3	92	40	31.30
4	94	44	31.46
5	98	51	31.93
6	108	63	35.09
7	117	76	36.08
8	133	Error	—

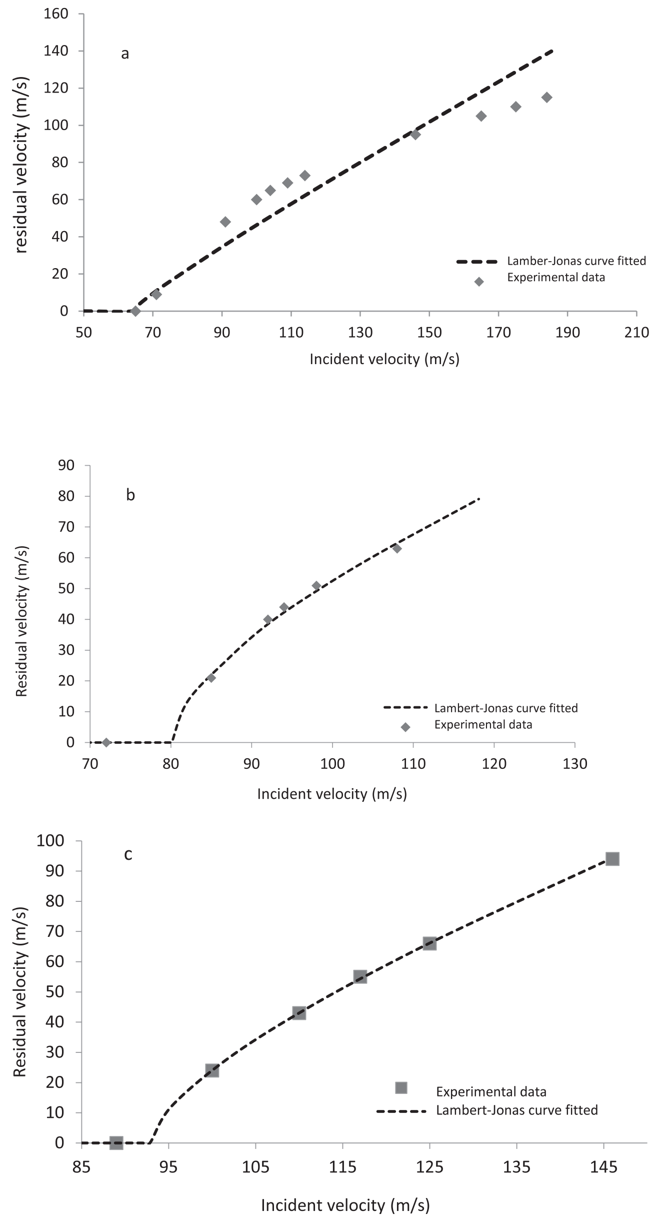

Figure 2.—Experimental residual velocity fitted with the Lambert-Jonas equation for solid wood (a), oriented strand board (b), and plywood (c).

As shown in Table 2, a higher E_{ab} was also observed for plywood. The higher energy absorption and the limit velocity of plywood could be as a result of its multilayered design. Figure 3 shows the changes in the percentage of energy absorption with increasing the initial velocity of the projectiles. The higher impact properties of plywood can be attributed to its high ultimate tensile strength, failure strain, and toughness in both directions. The low tensile properties of solid wood when loaded perpendicular to the grain

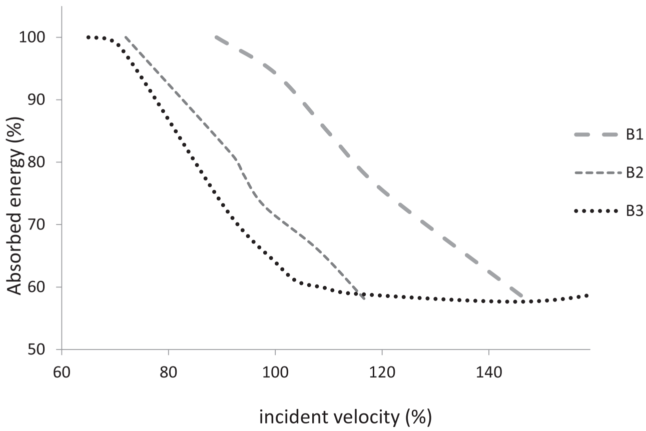

Figure 3.—The comparison of wood (B3), plywood (B1), and oriented strand board (B3) based on the percentage ratio of E_{ab} *to initial impact energy.*

direction were distractive for the energy absorption capability of wood.

As reported by Bekyarova et al. (2007), the damaged area is related to the impact energy and the material's response to the impact event. In high-velocity impacts, the response of the structural element is governed by the local behavior of the material in the neighborhood of the impacted zone. At high velocities, solid wood, plywood, and OSB hinder the projectile by absorbing kinetic energy following a variety of energy absorption mechanisms through the formation of new surfaces in the surroundings of the impacted area. As shown in Figure 4, the impact loading induced by the projectile led to local damage and shear cracking parallel to the grain direction in solid wood as an impact energy absorption mechanism in solid wood. However, in plywood and OSB composites, the damage area was approximately the same in the two different directions. The breakage area in plywood and OSB consisted of the pathway of the projectile motion (perforation region) and delamination of the back layer induced by stress concentration in some parts of adhesive having low mechanical properties. The delamination of the back layer was larger in OSB because pulling off a strand is easier than pulling off a layer, resulting in lower-impact energy absorption in OSB compared to plywood. The failure modes observed in plywood and OSB after perforation included ply fracture, fragmentation, and delamination. Apart from these mechanisms, bending and microscopic-scale deformation and collapse of wood cell polymers may take place (Easterling et al. 1999, Maloney and Paulapuro 1999). The probability of cell collapse near the impactor increased with increasing impact velocity (Cady et al. 2009).

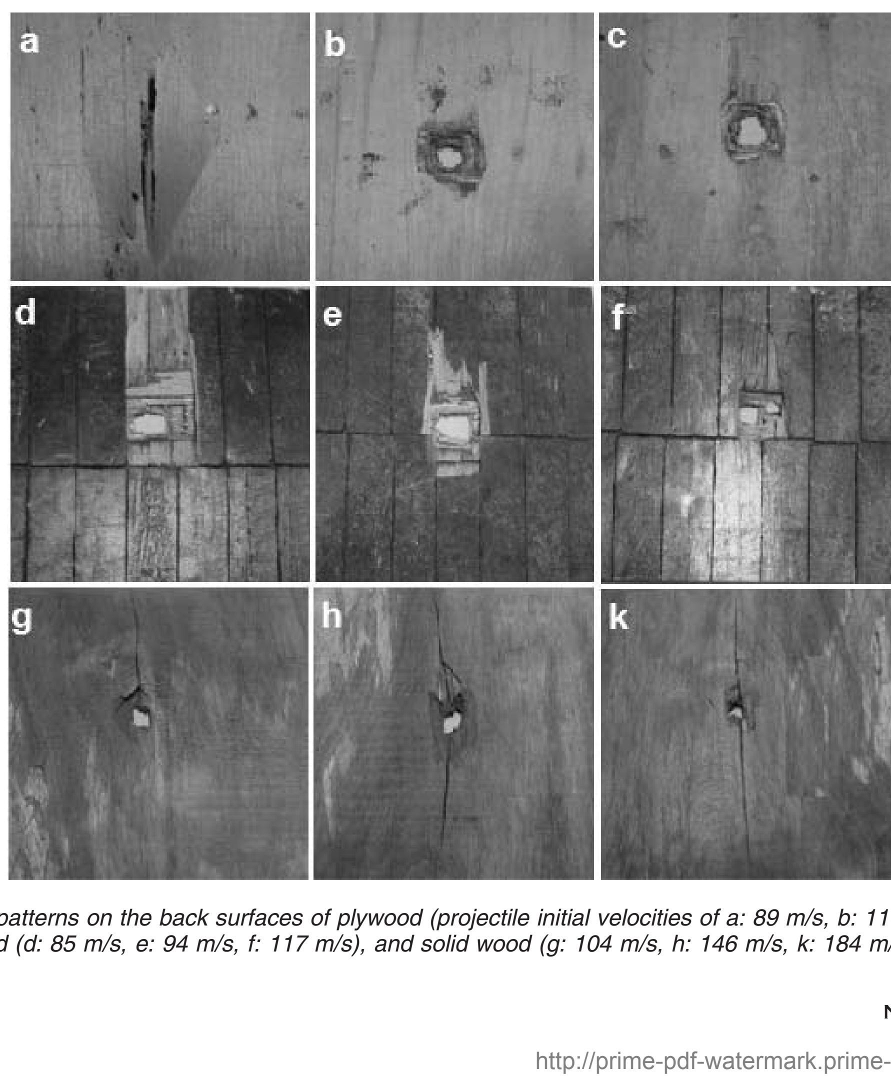

Figure 4.—Damage patterns on the back surfaces of plywood (projectile initial velocities of a: 89 m/s, b: 110 m/s and c: 125 m/s), oriented strand board (d: 85 m/s, e: 94 m/s, f: 117 m/s), and solid wood (g: 104 m/s, h: 146 m/s, k: 184 m/s).

Low-velocity impact

Velocity time response.—The time history of the velocity during the impact test with applied energy levels of 10 and 98 J is shown in Figures 5a and 5b. The negative velocity values represented upward motion due to striker rebound, while the positive values represented downward motion for the striker. The striker rebounded from wood, plywood, and OSB samples when 10 J energy was applied (Fig. 5a). The striker penetrated all the samples by applying 39, 78, and 98 J. Due to the higher stiffness of plywood, the rate of change in velocity is a bit higher compared to OSB and solid wood. The bounce point was defined as the point at which the striker's velocity approached zero (Fig. 5a). The upward velocity is the final velocity at the end of the impact event after the rebound of the striker. The bounce time and upward velocity also depend on the stiffness of the tested materials. Compared to OSB and wood, plywood samples showed lower bounce time, and their upward velocity was a little higher; however, the difference was not statistically significant.

The difference between initial and residual velocities, the penetration limit, in plywood is higher than in OSB and solid wood, as shown in Figure 6. For the applied energy of 98 J to plywood and OSB, increases of 46.66 and 18.89 percent, respectively, in penetration limit were observed over solid wood. Moreover, the penetration limit of plywood is 23.36 percent higher than OSB. The results show that as the applied energy decreases, the penetration limit increases.

Energy-time response.—Energy-time responses for solid wood, plywood, and OSB are shown in Figure 7 for the cases of 10, 39, 78, and 98 J. The penetration point, defined only above the penetration limit, is the point at which the force drops to 50 percent of the maximum or peak force according to the ISO 6603-2 standard (2000) (Fig. 8b). For applied energy of 98 J, an average of 238 and 125 percent improvement in penetration energy is observed for plywood and OSB, respectively, compared to solid wood. Moreover, the penetration energy of plywood is 49.79 percent higher than that of OSB because plywood is both stronger and more ductile relative to solid wood and OSB and withstands both higher stresses and higher strains, as shown in Table 1. So, the ability of plywood to absorb energy and plastically deform before fracturing is more than that seen in two other materials studied. Solid wood, when loaded perpendicular to the grain direction, exhibits low toughness and fails more easily by the impact of a projectile. Thus, for being an impact-resistant material, it is important to be tough in both directions independently, whether being tested parallel or perpendicular to the grain direction.

Load-displacement response.—Load-displacement responses for solid wood, plywood, and OSB subjected to various levels of energy of 10, 39, 78, and 98 J are shown in Figure 8. A difference in peak force was observed between the different cases studied. For applied energy of 98 J, an average of 29.69 and 8 percent increments in peak force is observed for plywood and OSB respectively, compared to solid wood. This maximum force shows the force needed to induce damage through material fracture and delamination. In solid wood, the load drops fast on reaching the maximum force, while in plywood and

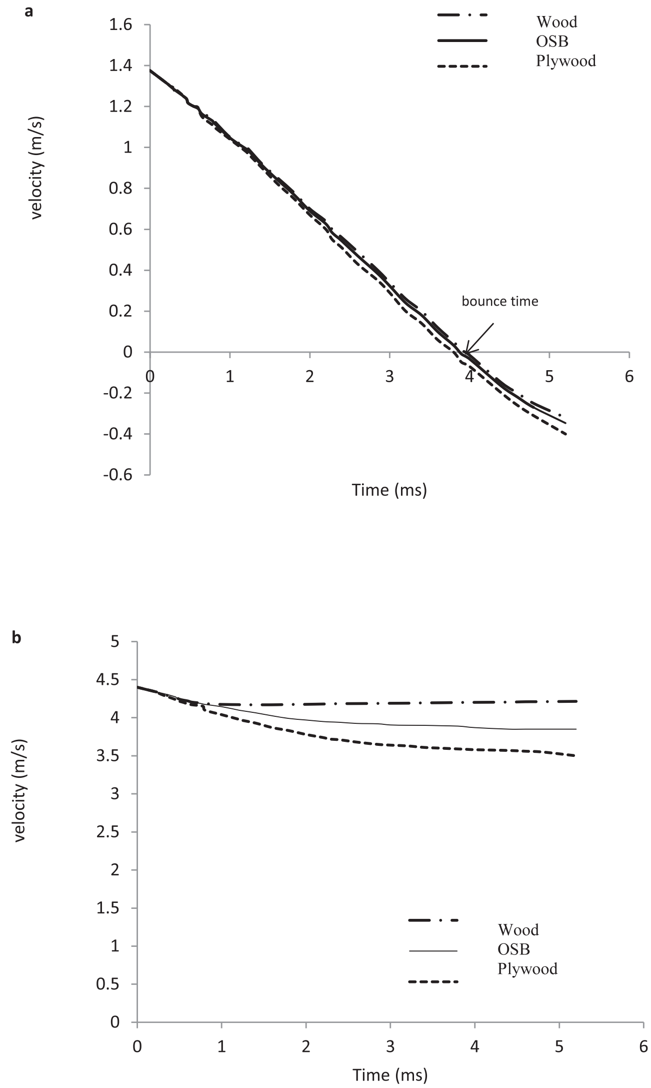

Figure 5.—Velocity-time response for materials subjected to (a) 10 J and (b) 98 J energy.

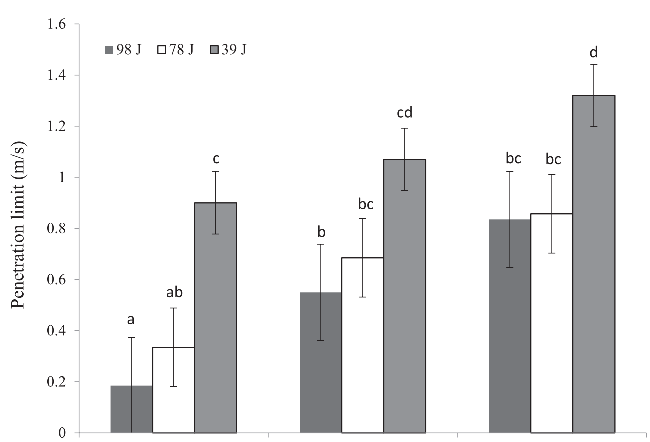

Figure 6.—Penetration limit of studied materials.

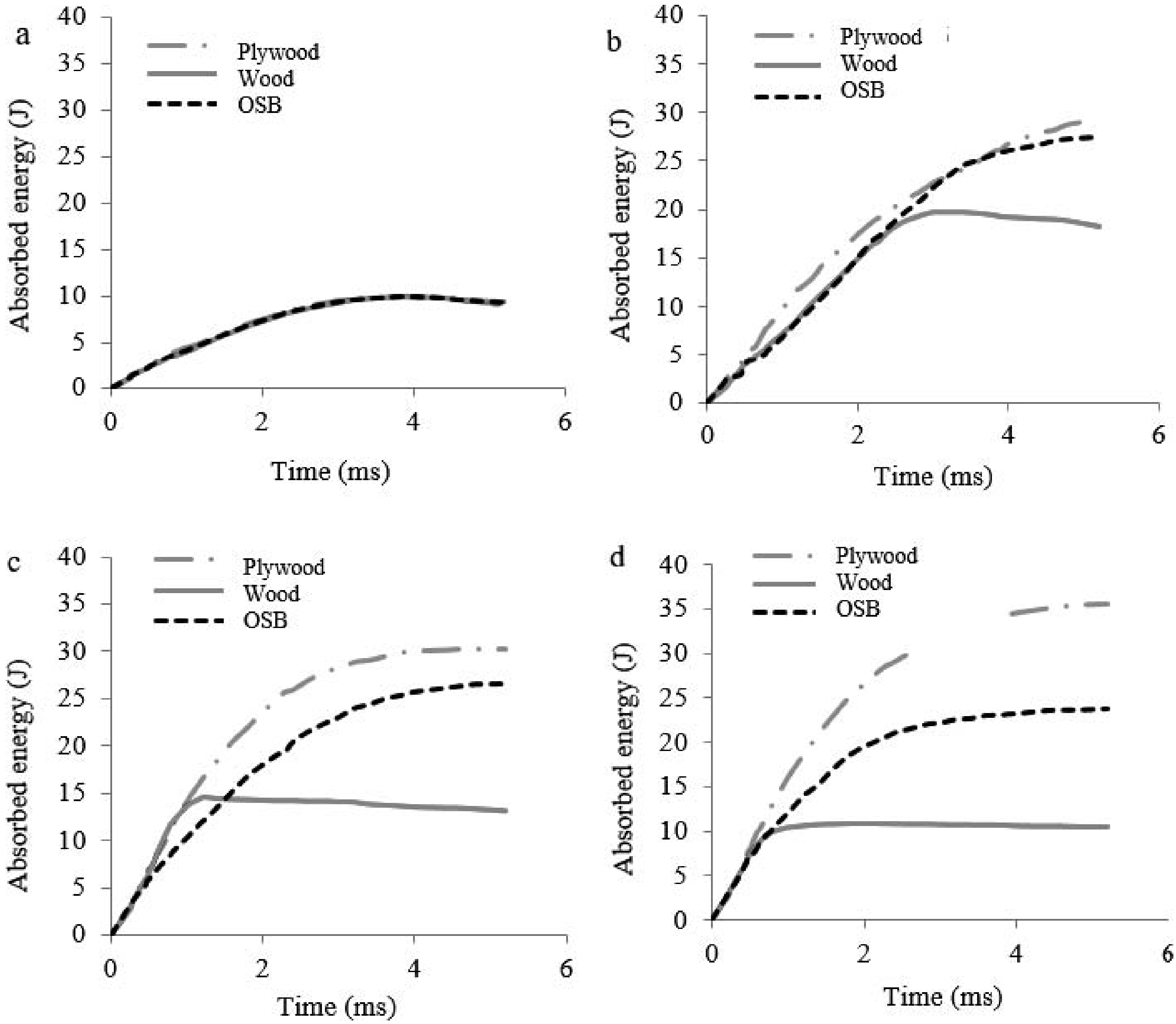

Figure 7.—Energy-time response for applied energies of (a) 10, (b) 39, (c) 78, and (d) 98 J.

especially OSB composites, the load deceased gradually. This can be attributed to the low shear strength of wood in transverse directions.

No significant differences were observed in bounce displacement of solid wood, plywood, and OSB. In contrast to the bounce displacements, studied materials have some influences in penetration displacement. For applied energy of 98 J, an average of 200 and 169 percent increments in penetration displacement was observed for plywood and OSB respectively, over solid wood. The penetration displacement increased by increasing applied energy, showing the higher strain capacity of plywood prior to fracture.

Damage evaluation.—Figure 9 shows the typical failure of studied materials. The fracture of the plywood and OSB involves delamination and ply fractures. While for solid wood fragmentation was the damage mechanism and with increasing the applied energy of striker, the number of fragments produced by impact increased. From Figure 9, it can be observed that the initial energy had a significant effect on damage size. In contrast to OSB, the damage size after the fracture of the plywood decreased with increasing applied energy. This could be explained by the ability of the plywood to absorb more energy than the OSB at lower energy levels. The higher energy absorption causes more damage and therefore increases the damage size.

Seventy, 81, and 93 percent energy was absorbed when the solid wood, OSB, and plywood were subjected to a high-velocity impact load of 39 J, respectively. However, for the low-velocity impact test, these showed 47, 71 and 75 percent energy absorption for the impact energy of 39 J, respectively. Therefore, in comparison to the quasi-static loading, the studied materials provided better performance under dynamic loading.

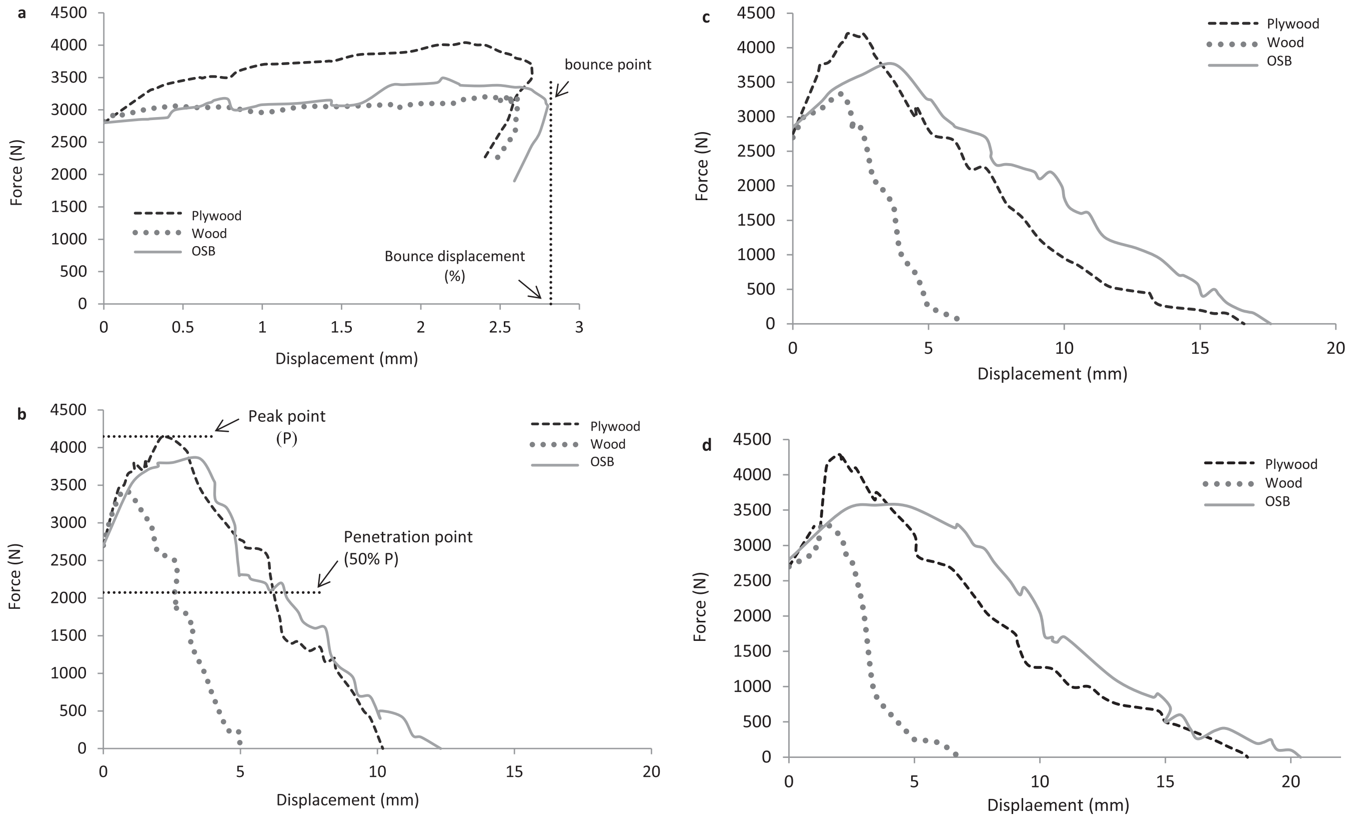

Figure 8.—Load-displacement response for applied energies of (a) 10, (b) 39, (c) 78, and (d) 98 J.

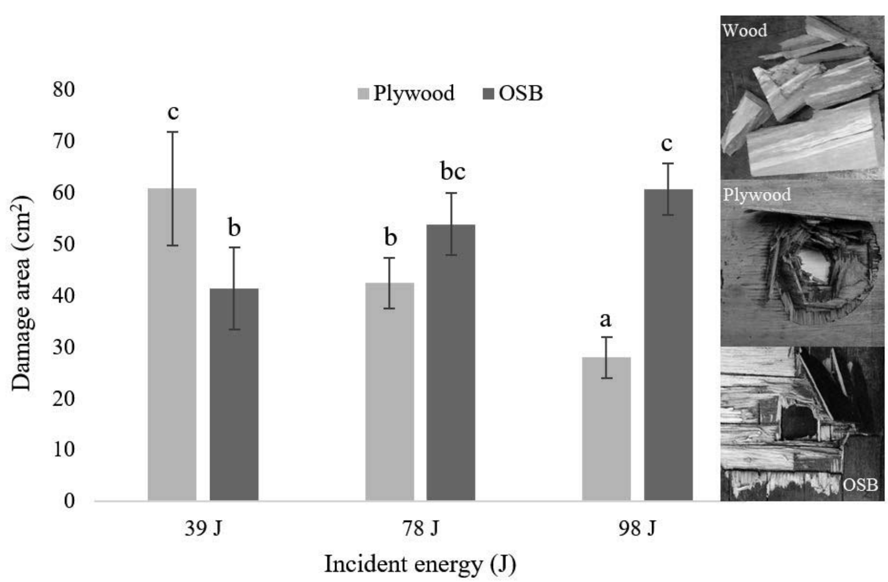

Figure 9.—Damage size for plywood and oriented strand board in different applied energies.

Conclusion

A series of low- and high-velocity impact tests has been conducted on solid wood, plywood, and OSB to evaluate their responses under widely differing loading conditions:

- For high-velocity impact loading by a fast-moving projectile at different velocities, a localized form of target response was induced. Plywood composites, under high-velocity impact loads, showed higher energy absorption and limit velocity compared to wood and OSB. However, the damage size in OSB composites indicated higher values.
- For conditions of low-velocity impact loading, lower-impact resistance has been observed in solid wood, whereas the highest-energy absorption capacity was seen in plywood.

- Compared to the low-velocity impacts, the studied materials provided better performance under high-velocity impact loading. The wooden materials are highly strain rate sensitive, especially in their tangential direction, and become stronger and stiffer under dynamic short-time loading.

Impact is a complex phenomenon, and future research should focus on understanding the effect of panel thickness and bond-line quality on impact performance of wooden materials at different strain rates.

Acknowledgments

The authors greatly acknowledge funding by the University of Tehran. We are also grateful to the Department of Mechanical Engineering, Tarbiat Modares University, for providing us with the high-velocity impact tester. The authors would like to thank the support provided by the Advanced Structure and Composites Center and the Department of Forestry, University of Maine.

Literature Cited

Aydin, I. 2004. Effects of some manufacturing conditions on wettability and bonding of veneers obtained from various wood species. PhD thesis. Karadeniz Technical University, Trabzon, Turkey. (In Turkish.)

Aydin, I. and G. Colakoglu. 2005. Effects of surface inactivation, high temperature drying and preservative treatment on surface roughness and color of alder and beech wood. *Appl. Surf. Sci*. 252(2):430–440.

Bekyarova, E., E. T. Thostenson, A. Yu A, H. Kim, J. Gao, J. Tang, H. T. Hahn, T.-W. Chou, M. E. Itkis, and R. C. Haddon. 2007. Multiscale carbon nanotube-carbon fiber reinforcement for advanced epoxy composites. *Langmuir* 23(7):3970–3974.

Cady, C. M., G. T. Gray, C. Liu, M. L. Lovato, and T. Mukai. 2009. Compressive properties of a closed-cell aluminum foam as a function of strain rate and temperature. *Mater. Sci. Eng. A* 525(1–2):1–6.

Deka, L. J. and U. K. Vaidya. 2008. LS-DYNA impact simulation of composite sandwich structures with balsa wood core. *In:* 10th International LS-DYNA Users Conference, June 8–10, 2008, Dearborn, Michigan; Livermore Software Technology Corporation, Livermore, California. pp. 13–23.

Douglas, H. 1860. A Treatise on Naval Gunnery. London: John Murray.

Easterling, K. E., R. Harrysson, L. J. Gibson, and M. F. Ashby. 1999) On the mechanics of balsa and other woods. *Proc. R. Soc. A* http://dx.doi.org/10.1098/rspa.1982.0118

Forest Products Laboratory. 2010. Wood Handbook—Wood as an Engineering Material. General Technical Report FPL-GTR-190. US Department of Agriculture, Forest Service, Forest Products Laboratory, Madison, Wisconsin.

ISO 6603-2 (2000) Plastics—Determination of puncture impact behaviour of rigid plastics—Part 2: Instrumented impact testing. European Standards National Standards Authority of Ireland, Dublin. pp. 1–3.

Johnson, W. 1986a. Mostly on oak targets and 19th century naval gunnery. *Int. J. Impact Eng*. 4(3):175–183.

Johnson, W. (1986b). Historical and present-day references concerning impact on wood. *Int. J. Impact Eng*. 4(3):161–174.

Lambert, J. P. and G. H. Jonas. 1976. Towards standardization of in terminal ballistics testing: Velocity representation. Report BRL-R-1852. Ballistic Research Laboratories, Aberdeen Proving Ground, Aberdeen, Maryland.

Maloney, T. C. and H. Paulapuro. 1999. The formation of pores in the cell wall. *J. Pulp Paper Sci*. 25:430.

Mehrabani Yeganeh, E., G. H. Liaghat, and M. H. Pol. 2016. Laminate composites behavior under quasi-static and high velocity perforation. *Steel Compos. Struct*. 22(4):777–796.

Naghizadeh, Z., M. Faezipour, M. M. Pol, G. H. Liaghat, and A. Abdolkhani. 2017. High velocity impact response of carbon nanotubes-reinforced composite sandwich panels. *J. Sandwich Struct. Mater.* https://doi.org/10.1177/1099636217740816

Otkur, A. M. 2010. Impact modeling and failure modes of composite plywood. Master's thesis. Texas Tech University, Lubbock.

Palamidi, E. and J. J. Harrigan. 2006. An investigation of balsa wood over a range of strain-rates and impact velocities. J. *Phys. IV France* 134:225–230.

Pol, M. H., G. H. Liaghat, and F. Hajiarazi. 2013. Effect of nanoclay on ballistic behavior of woven fabric composites: Experimental investigation. *J. Compos. Mater*. 1563–1573.

Polocoser, T., B. Kasal, and F. Stöckel. 2017. State-of-the-art: Intermediate and high strain rate testing of solid wood. *Wood Sci. Technol.* https://doi.org/10.1007/s00226-017-0925-6

Polocoser, T., F. Stockel, and B. Kasal. 2016. Low-velocity transverse impact of small, clear spruce and pine specimens with additional energy absorbing treatments. *J. Mater. Civ. Eng*. doi:10.1061/(ASCE)MT. 1943-5533.0001545

Reid, S. R. and C. Peng. 1997. Dynamic uniaxial crushing of wood. *Int. J. Impact Eng*. 19:531–570.

Task Committee on the State-of-the-Art. 1975. Wood Structures: A Design Guide and Commentary. American Society of Civil Engineers, New York.

Zike, S. and K. Kalnins. 2011. Enhanced impact absorbanced properties of plywood. *In:* Civil Engineering '11, Proceedings of the 3rd International Scientific Conference, May 12–13, 2011,, Jelgava, Latvia; University of Agriculture, Jelgava, Latvia, 3:125–130.